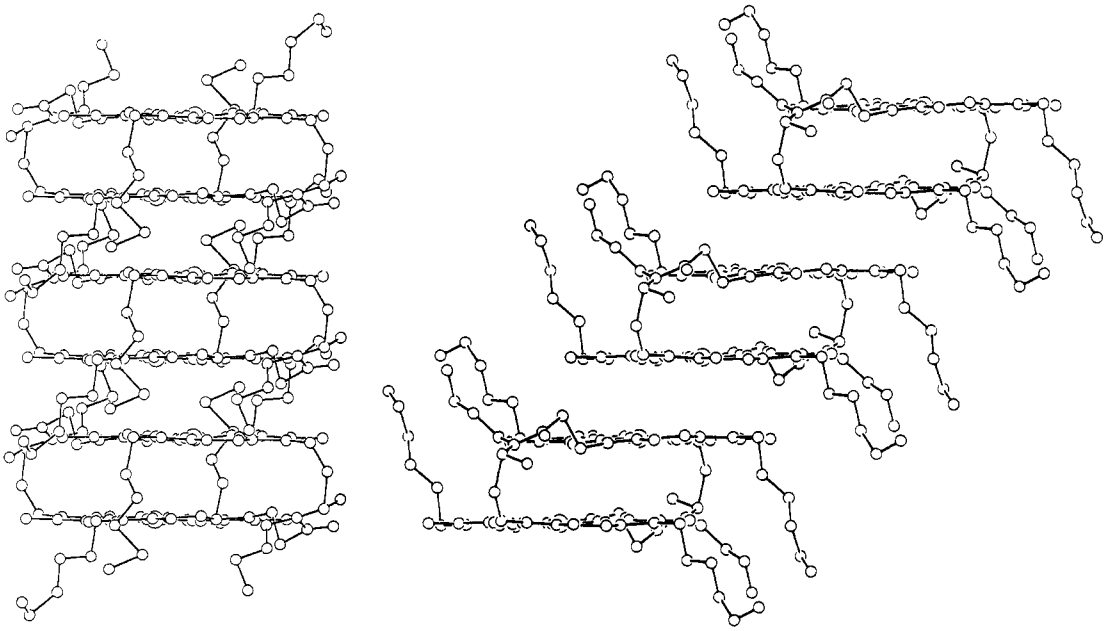

Figure 3. Stacking of Cu_2DP-7 along *b* axis. Views along ring directions and mutually perpendicular.

±1–2° in bond angles. The atomic parameters of Cu_2DP-7 have been deposited as supplementary material.[9]

A perspective ORTEP drawing of the structure of Cu_2DP-7 is shown in Figure 1 where the black circles represent the disordered carbonyl oxygen atoms of the porphyrin bridges. A least-squares plane calculation of the porphyrin ring, including the Cu atom, showed that it is planar within ±0.1 Å. The two porphyrin rings are not stacked exactly over each other, and the manner in which the rings slip is depicted schematically in Figure 2. From Figure 2, which shows the projection of the central core of one porphyrin onto that of the other, it can be seen that the slip of 3.80 Å corresponds closely to the methine–methine direction, giving a Cu–Cu distance of 5.22 Å. This also gives a slip angle of 43.2°.[10] When viewed perpendicular to the porphyrin rings, the projection of N2 is such that it nearly coincides with the center of the pyrrole ring below it while centrosymmetrically related N2 projects near the center of the pyrrole above it. The interplanar distance between rings is 3.52 ± 0.08 Å, corresponding to a normal van der Waals contact. The geometry of the immediate environment of the Cu atom is also shown in Figure 2 from which it can be seen to be square planar within the errors of the determination.

The *n*-hexyl chains of a given ring assume approximately centrically related extended configurations perpendicular to the ring giving rise to a number of close van der Waals contacts with hexyl chains of the opposite ring (Figure 1). The *n*-butyl chain of the carboxyamide group also has an extended and perpendicular configuration with respect to the porphyrin ring (Figure 1). This aliphatic side-chain structure in combination with the crystal packing leads to hydrocarbon channels in the crystal within which porphyrin rings are stacked (Figure 3). In fact, the interplanar distance between dimer molecules (3.47 ± 0.08 Å) is also normal van der Waals and is the same as that within a dimer, but, somewhat unexpectedly, the intermolecular Cu–Cu distance is less (4.60 Å) than the intramolecular distance. The latter results because there is less intermolecular slip (3.17 Å) between adjacent rings of dimer molecules (slip angle = 46.4°).

The disorder displayed by Cu_2DP-7 is unusual in that the three-carbon-atom aliphatic portions of the seven-atom bridges between porphyrin rings and the carboxamide half of the bridges have different configurations in the same molecule (Figure 1). Since these configurations are, except for the carbonyl oxygen, *centrosymmetrically* related in the dimer, the crystal is composed of dl enantiomorphs which leads *only* to disordered carbonyl oxygen atoms in the overall structure (Figure 1). This is dramatically borne out by the order displayed in the hexyl groups and *n*-butyl groups of this cofacial diporphyrin.

The slipped configuration of this Cu_2DP-7 may be a general structural feature of other metallodiporphyrins and free base diporphyrins. Preliminary results of a free base H_2DP-7 also show that the two rings are stacked with similar geometry.[11] The slipped configuration is certainly of significance for ligand intercalation; for example, dioxygen adducts to Co_2DP and Fe_2DP could also assume a slipped "trans" geometry. While direct X-ray structure proof of these complexes is still lacking, we have observed changes in EPR spectra and electrocatalytic behavior of the dicobalt system as we shortened the amide linking chains between the rings which physically limit the degree of slippage and vary the metal–oxygen bond geometry.[12]

The details of the structure determination will appear elsewhere.

Acknowledgments are made by C.K.C. to the donors of the Petroleum Research Fund, administered by American Chemical Society, and National Science Foundation (CHE-7815285) for partial support of this research.

Supplementary Material Available: Table of atomic parameters of Cu_2DP-7 and figure describing numbering system (3 pages). Ordering information is given on any current masthead page.

(9) See paragraph at end of paper regarding supplementary material.
(10) Slip angle = $\sin^{-1}$ (magnitude of slip/Cu–Cu distance).
(11) Unpublished results of this laboratory.
(12) A preliminary account was presented by C. K. Chang and C.-B. Wang at the Airlie House Symposium on "Interaction Between Iron and Proteins in Oxygen and Electron Transport", Airlie House, VA, April 1980; manuscript in preparation.

Marcos H. Hatada, A. Tulinsky,* C. K. Chang
Department of Chemistry
Michigan State University
East Lansing, Michigan 48824
Received June 2, 1980

Biomimetic Synthesis of Macroline[1]

Sir:

Much current interest in the later stages of indole alkaloid biogenesis[2] together with the search for simple and direct synthetic

(1) Dedicated to the memory of Robert C. Elderfield, 1904–1979.

0002-7863/80/1502-7116$01.00/0

approaches give impetus to biomimetic syntheses of these alkaloids. In previous work in our laboratory,[3] macroline (**1**) was shown to serve as a direct precursor of the bisindole alkaloids villalstonine, alstonisidine, macralstonine, and macralstonidine as well as of the monomeric base alstonerine and, by extension, alkaloids in the talcarpine series.

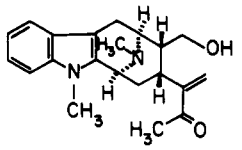

1

Macroline (**1**) itself has not been encountered as a natural product, which led us to propose[3] that it or an equivalent such as the β-ketoammonium salt (**2**), which would arise from a sarpagine-like structure, exists in low, steady-state concentrations on the biosynthetic pathways. We now report a synthesis of macroline (**1**) via a derivative of **2** which gives strong support for this biogenetic proposal.

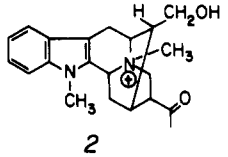

2

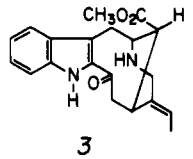

3

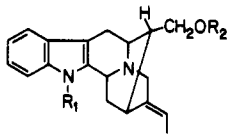

4 $R_1 = R_2 = H$
5 $R_1 = H$, $R_2 = SiMe_2t\text{-}Bu$
6 $R_1 = Me$, $R_2 = SiMe_2t\text{-}Bu$

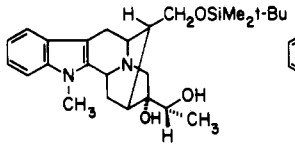

7

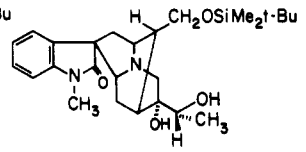

8

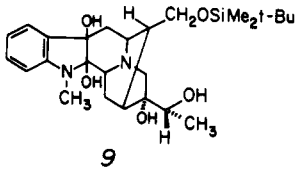

9

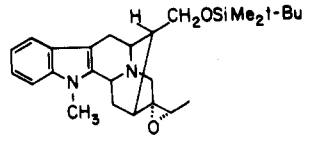

10

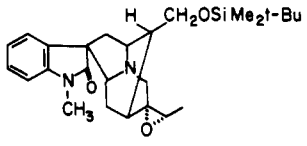

11

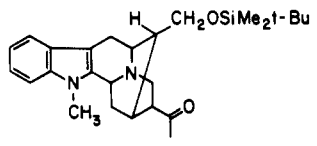

12

Perivine (**3**) was converted to normacusine B (**4**) by methods close to those previously reported.[4] The primary hydroxyl group of **4** was protected as the *tert*-butyldimethylsilyl ether **5**[5] (*t*-$BuMe_2SiCl$, imidazole, DMF), then converted to the N_a-methylated compound **6** (KH, NH_3/THF, MeI). Attempts to epoxidize the ethylidene double bond directly, with selectivity and in high yield, in the presence of the indole nucleus and tertiary nitrogen, either via hydroxyl-directed reagents[6] on normacusine B (**4**) or with other epoxidizing reagents on the silyl ether **6**, were unsuccessful.[7] However, osmylation of **6** (1.1 equiv of OsO_4 in THF/py, sodium metabisulfite workup) gave an inseparable mixture of the diol **7** and the spirooxindole **8**, the latter presumably arising from the tetrol **9** during chromatography of the crude mixture. The osmylation proceeded stereoselectively owing to the bulky *tert*-butyldimethylsilyl function blocking one side of the ethylidene group. The mixed diols **7** and **8** were tosylated (TsCl, py) and the tosylates converted to the epoxides **10** and **11** with NaH/THF. The desired epoxide **10** (one stereoisomer) could be separated cleanly by direct crystallization. Rearrangement of **10** (freshly prepared $MgBr_2$, refluxing Et_2O/benzene) gave the oily ketone **12** which with Me_2SO_4/K_2CO_3 (refluxing benzene, 18 h) followed by $Bu_4N^+F^-$ (THF/H_2O) gave only macroline (**1**), identical in all respects with material obtained by degradation of villalstonine.[8]

This work gives direct in vitro experimental support to the biogenetic hypothesis proposed earlier,[3] and implies that sarpaginelike structures such as normacusine B (**4**) are the precursors of all the macroline-related indole alkaloids.

Acknowledgment. We are very grateful to Dr. Gerald L. Thompson, Lilly Research Laboratories, for generous gifts of perivine.

(2) For a general review of this topic, see: Dalton, D. R. "The Alkaloids"; Marcel Dekker: New York, 1979; pp 432–479.
(3) Garnick, R. L.; Le Quesne, P. W. *J. Am. Chem. Soc.* **1978**, *100*, 4213, and references cited therein.
(4) Gorman, M.; Sweeney, J. *Tetrahedron Lett.* **1964**, 3105.
(5) All new compounds gave satisfactory analytical and spectral data.
(6) See, for example: Sharpless, K. B.; Michaelson, C. R. *J. Am. Chem. Soc.* **1973**, *95*, 6136.
(7) See, for example: Kutney, J. P.; Balserich, J.; Bokelman, G. H.; Hibino, T.; Honda, T.; Itoh, I.; Ratcliffe, A. H.; Worth, B. R. *Can. J. Chem.* **1978**, *56*, 62. Mimoun, H.; Seree de Roch, I.; Sajus, L. *Tetrahedron* **1970**, *26*, 37.
(8) Hesse, M.; Hürzeler, H.; Gemenden, C. W.; Joshi, B. S.; Taylor, W. I.; Schmid, H. *Helv. Chim. Acta* **1965**, *48*, 689.

Robert W. Esmond, Philip W. Le Quesne*

Department of Chemistry, Northeastern University
Boston, Massachusetts 02115

Received June 16, 1980

Use of Holography to Investigate Photochemical Reactions

Sir:

In order to monitor a photochemical reaction, it is necessary in some way to measure the disappearance of the reactants or the appearance of the products. A variety of techniques have been developed to accomplish this.[1] In perhaps the most frequently used technique, one follows changes in optical absorption of the reactants or products. The sensitivity of this kind of experiment is low because of the difficulties involved in detecting small absorption changes. Here, a new technique is described that allows one, in a very simple manner, to follow the course of the reaction by measuring the growth in intensity of a holographic image. This method is essentially a zero-background technique and has the high sensitivity characteristic of techniques of this type. Furthermore, since the intensity of the hologram depends not only on changes in the absorption coefficient but also on changes in

(1) Calvert, J. G.; Pitts, J. N. "Photochemistry"; Wiley: New York, 1966; pp 580–670.

0002-7863/80/1502-7117$01.00/0